Evolution of diversity in metabolic strategies

R. A. Caetano*
Departamento de Física - Universidade Federal do Paraná, Caixa Postal 19044, 81531-990, Curitiba, PR, Brazil

Y. Ispolatov
Departamento de Fisica, Universidad de Santiago de Chile Casilla 302, Correo 2, Santiago

M. Doebeli
Departments of Mathematics and Zoology, University of British Columbia, 6270 University Boulevard, Vancouver B.C. Canada, V6T 1Z4

(Dated: October 20, 2020)

Understanding the origin and maintenance of biodiversity is a fundamental problem. Many theoretical approaches have been investigating ecological interactions, such as competition, as potential drivers of diversification. Classical consumer-resource models predict that the number of coexisting species should not exceed the number of distinct resources, a phenomenon known as the competitive exclusion principle. It has recently been argued that including physiological tradeoffs in consumer-resource models can lead to violations of this principle and to ecological coexistence of very high numbers of species. Here we show that these results crucially depend on the functional form of the tradeoff. We investigate the evolutionary dynamics of resource use constrained by tradeoffs and show that if the tradeoffs are non-linear, the system either does not diversify, or diversifies into a number of coexisting species that does not exceed the number of resources. In particular, very high diversity can only be observed for linear tradeoffs.

I. INTRODUCTION

Life on Earth is spectacularly diverse [1]. For example, one study in the early 2000's found that the number of species of fungi is, by a conservative estimate, ca. 1.5 M [2]. However, the author revisited the same problem recently and re-estimated this number to something between 2.2 to 3.8 M species [3]. Microbes are by far the most diverse form of life. They constitute approximately 70-90% of all species [4]. The human gut alone houses hundreds of species of bacteria [5] that coexist in symbiosis and play an important role for human health. Perhaps even more astonishing than the number of species is the fact that all of them came from a single common ancestor [6–8]. To understand the fundamental mechanisms behind such diversification is one of the most relevant problems addressed by the scientific community [9–15].

Recently, ecological interactions, such as competition, have received a lot of attention as potentially very strong drivers of diversification and speciation. The theoretical framework of adaptive dynamics has become a powerful tool to study gradual evolutionary diversification due to frequency-dependent ecological interactions [13, 16–22]. In particular, adaptive dynamics can generate the paradigmatic phenomenon of evolutionary branching [13, 16, 19–22], during which a population that evolves in a continuous phenotype space first converges to a fitness minimum (evolutionary branching point) and then splits into two (or more) diverging phenotypic branches. A widely used class of models in which this phenomenon can be observed is based on classical Lotka-Volterra competition models, which are augmented by assuming that the carrying capacity is a (typically unimodal) function of a continuous phenotype, and the strength of competition between two phenotypes is measured by a competition kernel, which is typically assumed to be a (symmetric) function of the distance between the competing phenotypes, with a maximum at distance 0 (so that the strength of competition decreases with increasing phenotypic distance).

These assumptions are biologically plausible, and such models have been widely used to provide insights into evolutionary diversification due to competition [13, 23, 24]. However, these models are not derived mechanistically from underlying resource dynamics, and in fact it is known that the commonly used Gaussian functions for the carrying capacity and the competition kernel are not compatible with resource-consumer models [25, 26]. A more mechanistic approach is desirable. For example, it has recently been shown that adaptive dynamics derived from the classical MacArthur consumer-resource model [27] can in principle be very complicated [28].

Recently, a MacArthur model was studied in an ecological context with a view towards explaining the existence of very high levels of diversity [29]. The authors consider different species competing for R interchangeable resources, each of which is supplied at a constant rate. A consumer species is characterized by an uptake strategy, $\alpha = (\alpha_1, ..., \alpha_R)$, where the jth component $\alpha_j \geq 0$ represents the amount of cellular metabolism allocated to the uptake of the jth resource. The total amount of cellular metabolism available for resource uptake is lim-

* caetano@fisica.ufpr.br

ited, and hence it is natural to assume a tradeoff between the uptake rates of different resources. In general mathematical terms, a tradeoff is typically given by a function $T(\alpha) = T(\alpha_1, ..., \alpha_R)$ that is increasing in each of the arguments α_j, and such that the only permissible allocation strategies α are those satisfying $T(\alpha) \leq E$, where E is a constant. The analysis is then typically restricted to the subspace of strategies defined by $T(\alpha) = E$ (because T is increasing in each α_j).

It was shown in [29] that, under the assumption of a linear tradeoff, $\sum_j^R \alpha_j = E$, very high levels of diversity, i.e., many different species with different α-strategies, can coexist. This is a very interesting finding because it violates the competitive exclusion principle [30], according to which at most R different species should be able to coexist on R different resources. Such high levels of diversity emerging from simple consumer-resource models could help solve the paradox of the plankton [31] from an ecological perspective.

Here, we incorporate evolutionary dynamics into the ecological model of [29] and investigate the conditions under which diversity evolves from single ancestors. To make the model more general, we consider non-linear tradeoffs in resource use. Due to the general complexity of resource uptake machineries, investigating non-linear effects of allocation strategies appears to be a reasonable. For example, maintaining a variety of pathways to harvest all available resourses simultaneously could either be more energetically costly than focusing on just one resource due to incompatibility between corresponding metabolic processes. Or conversely, concentrating on an uptake of just one resource could result in a costly bottleneck of extreme specialization of corresponding transcription and translation machinery. In this paper, we incorporate non-linear effects into the tradeoff function by considering the energy budget as a sum $\sum_j^R \alpha_j^\gamma = E$, where γ and E are positive constants. We show that in the resulting evolutionary model, coexistence of more than R species only emerges for the (structurally unstable) linear case $\gamma = 1$. Using adaptive dynamics and numerical simulations, we show that regardless of the value of γ, an initially monomorphic population always evolves to a singular point, after which two generic scenarios are possible: *i)* if $\gamma < 1$, the population branches and diversifies, with the maximal number of coexisting species equal to the number of resources R, a state in which each species is a complete specialist on exactly one of the resources; *ii)* if $\gamma > 1$, an initially monomorphic population also evolves to a singular point, but subsequently does not diversify and instead remains a monomorphic generalist. Overall, our results show that very high levels of diversity do not evolve in the consumer-resource model considered here if tradeoffs in resource preference are non-linear.

II. MODEL AND RESULTS

We consider a population competing for R substitutable resources in well-mixed environments. Each resource is supplied to the system at a constant rate, defined by the supply vector $S = (S_1, \ldots, S_R)$, where S_j is the supply rate of the jth nutrient. A phenotypic species α is characterized by its metabolic allocation strategy $\alpha = (\alpha_1, \ldots, \alpha_R)$, where α_j is the per capita rate at which individuals of species α take up the jth nutrient From a physiological perspective, α_j is proportional to the amount of metabolic effort allocated by the individuals of species α to capture nutrient j. Intrinsic limitations on metabolic activities impose a restriction on the total amount of nutrient uptake. For simplicity, we assume that this intrinsic limitation leads to a tradeoff in the components α_j of the form

$$\sum_{j=1}^{R} \alpha_j^\gamma = E, \tag{1}$$

where E and γ are positive parameters. (Note that we also assume $\alpha_j \geq 0$ for all j.) Throughout, we will set the scaling parameter $E = 1$. (See Supplementary Material for a more general treatment, in which the exponent γ can differ for different directions α_j in phenotype space.)

Following [29], we denote by $c_j(t)$ the concentration of resource j at time t, and we assume that the amount of resource j available for uptake per individual (e.g., the amount of resource bound to the outer membrane of a microbial cell) is given by a monotonously increasing function $r_j(c_j)$. Specifically, we assume this function to be of Monod type, $r_j(c_j) = c_j/(K_j + c_j)$ (any monotonically increasing and continually differentiable function with $r_j(0) = 0$ could be considered). Thus, the rate of uptake of resource j by an individual consumer with uptake strategy α is $\alpha_j r_j(c_j)$.

We further assume that resource j is supplied at a constant total rate S_j and decays at a rate μ_j. This generates the following system of equations for the ecological dynamics of the concentrations c_j, $j = 1, ..., R$:

$$\frac{dc_j}{dt} = S_j - \left(\sum_\alpha n_\alpha(t)\alpha_j \right) r_j(c_j) - \mu_j c_j. \tag{2}$$

Here $n_\alpha(t)$ is the population density of species α at time t, so that $(\sum_\alpha n_\alpha(t)\alpha_j)$ is the total amount of metabolic activity invested into uptake of resource j (the sum runs over all species α present in the community).

To derive the ecological dynamics of n_α, we assume as in [29] that metabolic reactions occur on a much faster time scale than cellular division, so that resource concentrations are always at their ecological equilibrium values c_j^* determined as solutions of equations (2) with $dc_j/dt = 0$. (Note that these equilibrium resource concentrations are determined by the current populations sizes $n_\alpha(t)$.) We further assume that the cellular per

capita growth rate of species α are proportional to the amount of nutrient absorbed by each individual,

$$g_\alpha(c_1^*, ...c_R^*) = \sum_j^R \alpha_j r_j(c_j). \tag{3}$$

The per capita death rates d are assumed to be the same for all consumers. The dynamics of the population size n_α then becomes

$$\frac{dn_\alpha}{dt} = (g_\alpha(c_1^*, ...c_R^*) - d)\, n_\alpha. \tag{4}$$

To derive the evolutionary dynamics for the allocation strategies, i.e., for the trait α, we follow the adaptive dynamics approach by considering a monomorphic resident population at its ecological equilibrium n_α^*, which is defined as the population size for which the equilibrium resource levels c_j^* are such that $g_\alpha(c_1^*, ..., c_R^*) = d$ (note again that the $(c_1^*, ..., c_R^*)$ implicitly depend on α). The invasion fitness of a rare mutant α' is then the per capita growth rate of the mutant α' at the resource levels defined by the resident:

$$f(\alpha, \alpha') = g_{\alpha'}(c_1^*, ...c_R^*) - d. \tag{5}$$

To derive the adaptive dynamics, we consider the selection gradient $q(\alpha) = (q_1(\alpha), ..., q_R(\alpha))$, with components

$$q_i(\alpha) = \frac{\partial f(\alpha, \alpha')}{\partial \alpha_i'}|_{\alpha'=\alpha}. \tag{6}$$

$q(\alpha)$ defines an R-dimensional dynamical system in unrestricted α-space,

$$\frac{d\alpha_i}{dt} = \sigma n_\alpha^* q_i(\alpha). \tag{7}$$

The speed of evolution of α is proportional to the current ecological equilibrium population size n_α^* because the number of mutations occurring at any given point in time is proportional to n_α^*. The parameter σ describes both the per capita rate and effective size of mutations. Without loss of generality, we set $\sigma = 1$.

To take the enzymatic tradeoff into account, the unconstrained adaptive dynamics (7) needs to be restricted to the surface in α-space that is defined by the tradeoff (1) [32]. For technical details we refer to the Supplementary Material.

Equilibrium points of the adaptive dynamics, so-called singular points, are resting points α^* of the resulting dynamical system in phenotype space. Given a singular point α^*, two stability concepts are important. First, there is stability in the usual sense of converging to α^* from nearby initial conditions, which is measured by the Jacobian matrix of the functions defining the adaptive dynamics, evaluated at α^* (see Supplementary Material). Second, evolutionary stability is measured by the Hessian of the invasion fitness function $f(\alpha^*, \alpha')$ with respect to the mutant trait and evaluated at the singular point α^*, and taken along the constraint surface [32]. A singular point is called an evolutionary branching point if it is both convergent stable with regard to the Jacobian and evolutionarily unstable with regard to the Hessian. Thus, a singular point is a branching point if all eigenvalues of the Jacobian have negative real parts, and if the Hessian matrix is not negative definite.

For the model presented above, analytical results are only available for a simplified system in which the resource decay rates μ_j are assumed to be 0 (as in [29]). In this case, there is a unique singular point determined by $d\alpha/dt = 0$,

$$\alpha_j^* = \left(\frac{S_j}{\sum_k S_k}\right)^{\frac{1}{\gamma}} \tag{8}$$

(see Supplementary Material). Calculations of the Jacobian of adaptive dynamics and of the Hessian of the invasion fitness function (see Supplementary Material) yield the following conclusions in terms of the exponent γ defining the metabolic tradeoff. Regardless of the value of γ, the singular point α^* is always convergent stable, so that the system approaches α^* from any initial condition. If $\gamma > 1$, the singular point α is also evolutionarily stable and hence represents the evolutionary endpoint. In particular, no diversification takes place. On the other hand, if $\gamma < 1$, the singular point is evolutionarily unstable, and hence is an evolutionary branching point. In particular, if $\gamma < 1$ the system will diversify into a number of coexisting consumer species. If $\gamma = 1$ (linear tradeoff), the fitness Hessian is 0, representing evolutionary neutrality.

To check our analytical approximations and to investigate the details of diversification after convergence to an evolutionary branching point, we performed numerical simulations that mimic evolution of populations consisting of multiple phenotypic strains. We numerically integrate the system of population dynamics equations (4) for M populations using a simple Euler update ($M = 1$ at the beginning of the simulations). After each integration step, the populations that fall below a small "extinction" threshold density (normally $n_{min} = 10^{-5}$) are removed from the system. The resource concentrations c_i and uptake rates r_i are considered relaxed to their steady states for a given set of populations $\{n_\alpha\}$,

$$r_i = \frac{(S_i + \phi_i + \mu_i K_i) - \sqrt{(S_i + \phi_i + \mu_i K_i)^2) - 4\phi_i S_i}}{2\phi_i}, \tag{9}$$

where $\phi_i = \sum_\alpha n_\alpha \alpha_i$. In the following numerical examples we considered a symmetric supply of resources $S_i = 1$ and a slow resource degradation, $\mu_i K_i = 0.1$

To mimic mutations, periodically (typically once every $\Delta t_{mutation} = 1$ time units) a mutant is split from an ancestor, which is randomly chosen with probability proportional to its total birth rate. The mutant's phenotype is slightly offset from the ancestral phenotype along the constraint surface. The offset distance is drawn from a uniform distribution in the interval $[-m, m]$. Unless otherwise noted, $m = 0.005$. The mutant population is set to

be 10% of the ancestral one, and the ancestor population is reduced by 10%. In addition to mutations, periodically (typically once every $\Delta t_{merge} = 100\Delta t_{mutation}$ time units) populations that are within a distance m of each other are merged (preserving their phenotypic center of mass) and their population sizes added. Periodic repetition of mutation and merging procedures preserves the phenotypic variance necessary for evolution while limiting computational complexity.

The procedure produces clouds or clusters of α-values in phenotype space (see figures), with each phenotype α representing a monomorphic population of individuals with that phenotype. Somewhat imprecisely, we refer to a distinct cluster of phenotypes as a species. The clusters move in phenotype space due to extinction and merging of phenotypes, and due to creation of new phenotypes by mutation. This movement represents evolution and occurs along the constraint surface. A diversification event occurs when a cluster corresponding to the diversifying species spontaneously splits into two or more clusters that diverge from each other and move apart.

Our numerical procedure can be applied to an evolving system of populations with any number of resources. To facilitate visualization, in the following we consider just three resources, so that because of the constraint, each population is characterized by two independent parameters α_i. In the figures below we show evolving populations as circles with radii proportional to square root of population size n_α and coordinates $(\alpha_1, \alpha_2, \alpha_3)$, viewed orthogonally to the simplex plane $\sum_{i=1}^{3} \alpha_i = 1$. When constraints are non-linear, $\sum_{i=1}^{3} \alpha_i^\gamma = 1$, the coordinates of each population are $(\alpha_1^\gamma, \alpha_2^\gamma, \alpha_3^\gamma)$.

To illustrate the results from numerical simulations, we first consider scenarios with linear tradeoffs, $\gamma = 1$. Figure 1 shows the time evolution of a population (shown in blue circles) whose individuals die at constant rate $d = 1$ (corresponding videos of the simulations can be accessed through the links provided in the figure legends). The black circle represents the singular point that is calculated in the limit of low degradation of nutrients, given by Eq. (8). Figure 1 (a) shows the initial monomorphic population far from the singular point. An intermediate time of the evolutionary process is shown in Figure 1 (b), in which the population remains monomorphic and is approaching the singular point. For $\gamma = 1$, the singular point is neutral evolutionarily (all eigenvalues of the Hessian of the invasion fitness function are 0 due to the linearity of the tradeoff), and once the population converges to the singular point, it starts to diversify "diffusively", as anticipated in [29]: neutrality of selection results in communities consisting of a large number of species. Thus, the high diversity observed in this case is an evolutionary consequence of the selective neutrality caused by a linear enzymatic trade-off.

The situation changes for non-linear tradeoffs, $\gamma \neq 1$, which generates two very different evolutionary regimes depending on whether $\gamma > 1$ or $\gamma < 1$ (even when the deviation of γ from one is fairly small). Figure 2 (a-c) shows an example of the evolutionary dynamics for $\gamma = 1.1$.

The dynamics starts with an initial monomorphic population far from the singular point, as shown in Figure 2 (a). As in the linear case, and as predicted by the analytical theory, the monomorphic population converges toward the singular point Figure 2 (b). However, because $\gamma > 1$ the singular point is evolutionarily stable, and no diversification occurs (apart from mutation-selection balance around the singular point). Instead, when the population reaches the singular point, evolution comes to a halt, and all individuals are generalists, i.e, use all resources to some extent (as determined by the location of the singular point), as depicted in Figure 2 (c).

On the other hand, Figure 3 (a-c) shows the evolutionary process for a community with $\gamma = 0.9$. The initial configuration is shown in Figure 3 (a). As in the previous examples, the initial phase of evolution ends with the population converging to the singular point. However, in this case, the singular point is an evolutionary branching point giving rise to the emergence of distinct and diverging phenotypic clusters (Figure 3 (b)). The final state of the evolutionary process is shown in Figure 3 (c): there are three coexisting phenotypic clusters, each of which is a specialist on exactly one of the resources. Our numerical simulations indicate that the results shown in Figs. 1-3 are general and robust: non-neutral diversification occurs only for $\gamma < 1$ and typically leads to coexistence of R specialists. In fact, the results easily generalize to situations in which the exponent γ in the tradeoff function may be different for different directions in phenotype space, i.e., for different α_j. As we show in the Supplementary material, evolutionary branching along a direction α_j in phenotype space can occur if the corresponding exponent $\gamma_j < 1$. Figures S1 and S2 in the supplementary material illustrate scenarios in which only a subset of the phenotypic directions α_j are branching directions along which evolutionary diversification occurs. In such case, the number of distinct species resulting from the evolutionary process is less than R.

Finally, we note that our results for the effects of non-linear tradeoffs on evolutionary dynamics have corresponding results in purely ecological scenarios, such as those studied in [29]. In fact, we can easily simulate ecological time scales by initiating the simulations with a set of e.g. randomly chosen phenotypes throughout phenotype space and then run the system with the mutational process turned off. Again, non-linear tradeoffs have a profound effect on the number of surviving species in such ecological simulations, with many species coexisting when $\gamma = 1$, as reported in [29], but with typically only R species surviving when $\gamma < 1$ and only very few species surviving in the close vicinity of the singular point when $\gamma > 1$. Figure S3 in the supplementary material illustrates these findings.

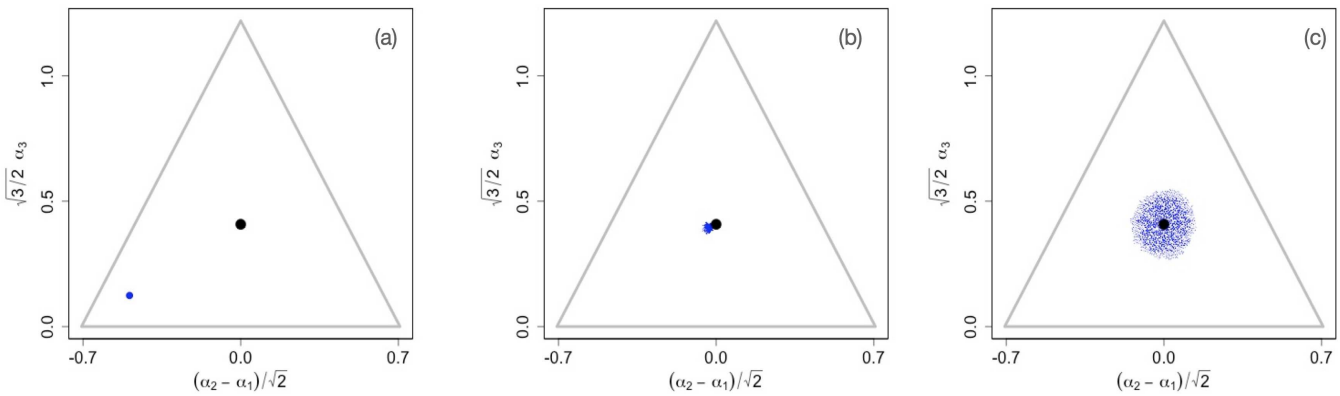

FIG. 1: Snapshots illustrating the beginning, intermediate, and advanced stages of evolution under a linear constraint, $\gamma = 1$. A video of the entire evolutionary process can be found **here**, frames are recorded every 200 time units until $t = 30000$ and then, to better illustrate slow neutral evolution, the frame recording time t_i were defined as a geometric progression $t_{i+1} = 1.006t_i$. Other parameter values were $S_j = 1$, $\mu_j K_j = 0.1$ for $j = 1, 2, 3$, and $d = 1$,

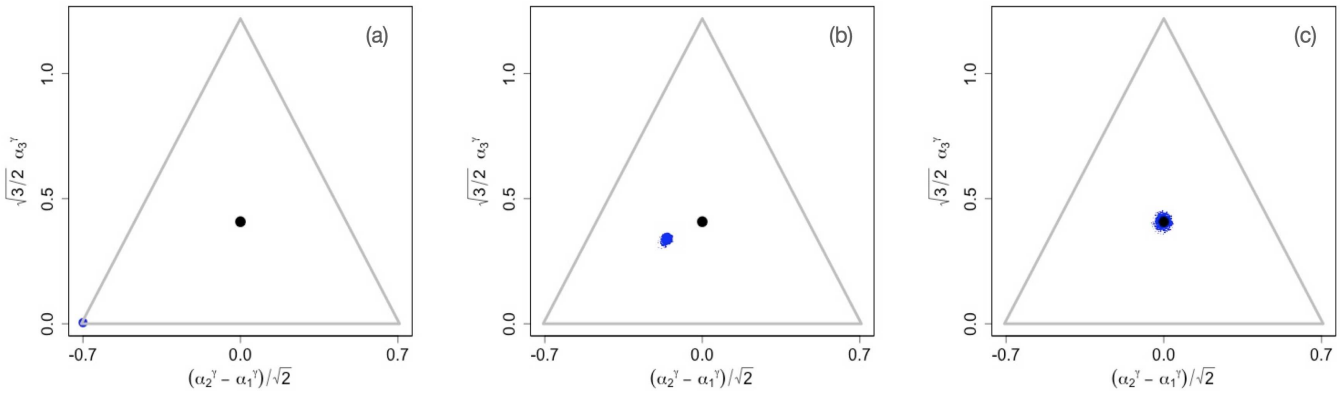

FIG. 2: Example of evolutionary dynamics for $\gamma = 1.1$, showing convergence to the singular point given by Eq. (8) (and indicated by the black dot), but no subsequent diversification. The corresponding video can be found **here**, each frame in the video is separated by 1000 time steps. Other parameter values were $S_j = 1$, $\mu_j K_j = 0.1$ for $j = 1, 2, 3$, and $d = 0.25$

III. CONCLUSIONS

To understand the origin and maintenance of diversity is a fundamental question in science. In particular, the mechanisms of diversification due to ecological interactions still generate lively debates. Recently, tradeoffs in metabolic activity for the uptake of different resources were suggested as a mechanism to generate large amounts of diversity [29], possibly solving the "paradox of the plankton" [31], and violating the competitive exclusion principle [30], which states that the number of coexisting species should not exceed the number of resources. It has recently been shown that enzymatic allocation strategies that are plastic instead of fixed, so that individuals can change their allocation (while maintaining a linear tradeoff under a fixed allocation budget) in response to resource availability during their life time, tend to reduce the amount of diversity maintained in the ecological communities [37]. Perhaps this is not surprising, since more plastic strategies tend to be able to be more generalist as well. As in [29], here we consider the case of non-plastic strategies, in which each individual is defined by its allocation vector α, but assuming more general nonlinear form of tradeoffs. Moreover, we investigate evolutionary rather than just ecological dynamics to determine the conditions under which evolutionary diversification can occur.

Because there are no true jacks-of-all trades in biology, tradeoffs are a ubiquitous assumption in evolutionary thinking and modeling. However, the cellular and physiological mechanisms that underly such trade-

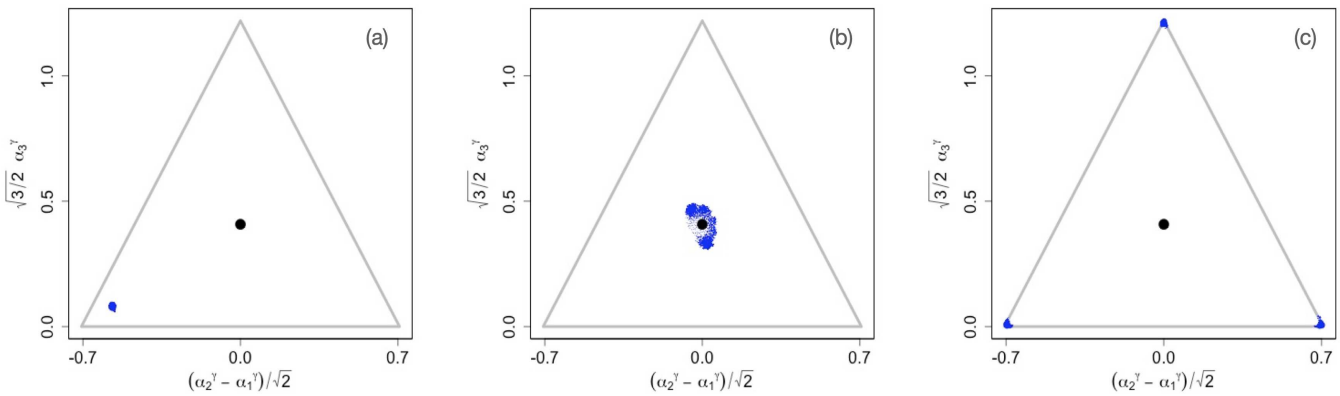

FIG. 3: Example of evolutionary dynamics for $\gamma = 0.9$, showing initial convergence to the singular point (indicated by the black dot) and subsequent diversification into three specialists, each consuming exclusively one of the three resources. The corresponding video can be found **here**, each frame in the video is separated by 1000 time steps. Other parameter values were $S_j = 1$, $\mu_j K_j = 0.1$ for $j = 1, 2, 3$, and $d = 0.25$,

offs are typically very complicated and the result of interaction chemical interactions between many different metabolic pathways. Attempts have been made to understand tradeoffs more mechanistically, particularly in microbes [48], but higher-level modeling efforts most often still require a mostly phenomenological approach to incorporating tradeoffs. In this paper we assumed that each of R resources is available to each microbial organism at a certain rate that depends on the resource concentration in the system. The microbe in turn is described phenotypically by the metabolic allocation that it makes to the uptake of the available resources. Without tradeoffs, and everything else being equal, the best strategy would be to allocate an infinite amount (or at least the maximal amount possible) of metabolic activity to every resource, a scenario that is generally unrealistic biologically. Rather, tradeoffs inherent to cell metabolism prevent such strategies. Formally, tradeoffs are given by one or more equations (or more generally inequalities) that the phenotypes of individuals have to satisfy.

In our simplistic models, tradeoffs are determined by the parameter γ, which essentially describes the curvature of the tradeoff function, with the linear tradeoff $\gamma = 1$ being the threshold between concave ($\gamma < 1$) and convex ($\gamma > 1$) tradeoffs. Formally, linear tradeoffs are the simplest case, but there is no a priori general reason why tradeoffs should be linear. Even for a single resource, the metabolic energy required for a given amount of enzymatic allocation to resource uptake may typically be a non-linear function of that allocation.

Our results show that generically, diversity only evolves with concave tradeoffs, and the number of coexisting species never exceeds the number of resources. Only in the structurally unstable linear case ($\gamma = 1$) is it possible for very high levels of diversity to evolve due to the cessation of selection at the evolutionary equilibrium. Any value of $\gamma \neq 1$ precludes high amounts of diversity. Extensive numerical explorations revealed that these results are robust and qualitatively independent of particular parameter choices, such as the number of resources.

It is well-known that the shape of tradeoff curves is, in general, an important component in adaptive dynamics models [44, 45]. Here we have the importance of the tradeoff curvature for the evolution and maintenance of diversity in a general consumer-resource model. Generic curvatures do not generate high levels of diversity, and instead the outcomes are in line with classical results about the evolution of resource generalists vs. resource specialists [46]. Of course, many potentially important ingredients that could yet lead to high diversity in these models were not considered in the present work. In particular, cross-feeding has recently been suggested as a key factor that could potentially enable such diversity [42]. In fact, [47] have extended their earlier models to more complicated ecological scenarios in the form of batch culture (rather than chemostat) dynamics, and including cross-feeding. They find that diversity can be affected in various ways, but they still only considered linear tradeoffs. It will be interesting to consider these model extensions with non-linear tradeoffs.

[1] R. M. May, How many species are there on earth?, Science **241**, 1441 (1988).
[2] D. L. Hawksworth, The magnitude of fungal diversity: the 1.5 million species estimate revisited, Mycological Research **105**, 1422 (2001).
[3] D. L. Hawksworth and R. Lcking, Fungal diversity revis-

ited: 2.2 to 3.8 million species, in *The Fungal Kingdom* (John Wiley & Sons, Ltd, 2017) Chap. 4, pp. 79–95.
[4] B. B. Larsen, E. C. Miller, M. K. Rhodes, and J. J. Wiens, Inordinate fondness multiplied and redistributed: the number of species on earth and the new pie of life, The Quarterly Review of Biology **92**, 229 (2017).
[5] F. Guarner and J.-R. Malagelada, Gut flora in health and disease, The Lancet **361**, 512 (2003).
[6] C. Darwin, *On the Origin of Species by Means of Natural Selection* (Murray, London, 1859) or the Preservation of Favored Races in the Struggle for Life.
[7] M. Steel and D. Penny, Common ancestry put to the test, Nature **465**, 168 (2010).
[8] D. L. Theobald, A formal test of the theory of universal common ancestry, Nature **465**, 219 (2010).
[9] E. Mayr and A. Mayr, *Animal Species and Evolution*, Belknap Press (Belknap Press of Harvard University Press, 1963).
[10] J. A. Coyne, Genetics and speciation, Nature **355**, 511 (1992).
[11] W. R. Rice and E. E. Hostert, Laboratory experiments on speciation: What have we learned in 40 years?, Evolution **47**, 1637 (1993).
[12] M. Higashi, G. Takimoto, and N. Yamamura, Sympatric speciation by sexual selection, Nature **402**, 523 (1999).
[13] U. Dieckmann and M. Doebeli, On the origin of species by sympatric speciation, Nature **400**, 354 (1999).
[14] S. Gavrilets and D. Waxman, Sympatric speciation by sexual conflict, Proceedings of the National Academy of Sciences **99**, 10533 (2002).
[15] M. A. M. de Aguiar, M. Baranger, E. M. Baptestini, L. Kaufman, and Y. Bar-Yam, Global patterns of speciation and diversity, Nature **460**, 384 (2009).
[16] J. Metz, R. Nisbet, and S. Geritz, How should we define fitness for general ecological scenarios?, Trends in Ecology & Evolution **7**, 198 (1992).
[17] U. Dieckmann and R. Law, The dynamical theory of coevolution: a derivation from stochastic ecological processes, Journal of Mathematical Biology **34**, 579 (1996).
[18] M. Doebeli and U. Dieckmann, Speciation along environmental gradients, Nature **421**, 259 (2003).
[19] M. Doebeli and U. Dieckmann, Evolutionary branching and sympatric speciation caused by different types of ecological interactions., The American Naturalist **156**, S77 (2000).
[20] C. Hui, H. O. Minoarivelo, and P. Landi, Modelling coevolution in ecological networks with adaptive dynamics, Mathematical Methods in the Applied Sciences **41**, 8407 (2018).
[21] M. Doebeli, *Adaptive Diversification (MPB-48)* (Princeton University Press, 2011).
[22] S. A. H. Geritz, J. A. J. Metz, E. Kisdi, and G. Meszéna, Dynamics of adaptation and evolutionary branching, Phys. Rev. Lett. **78**, 2024 (1997).
[23] M. Doebeli and I. Ispolatov, Continuously stable strategies as evolutionary branching points, Journal of Theoretical Biology **266**, 529 (2010).
[24] M. Doebeli and I. Ispolatov, Diversity and coevolutionary dynamics in high-dimensional phenotype spaces, The American Naturalist **189**, 105 (2017).
[25] P. A. Abrams, Character displacement and niche shift analyzed using consumer-resource models of competition, Theoretical Population Biology **29**, 107 (1986).
[26] M. Ackermann and M. Doebeli, Evolution of niche width and adaptive diversification, Evolution **58**, 2599 (2004).
[27] R. Macarthur and R. Levins, The limiting similarity, convergence, and divergence of coexisting species, The American Naturalist **101**, 377 (1967).
[28] I. Ispolatov and M. Doebeli, A note on the complexity of evolutionary dynamics in a classic consumer-resource model, Theoretical Ecology **13**, 79 (2020).
[29] A. Posfai, T. Taillefumier, and N. S. Wingreen, Metabolic trade-offs promote diversity in a model ecosystem, Phys. Rev. Lett. **118**, 028103 (2017).
[30] G. Hardin, The competitive exclusion principle, Science **131**, 1292 (1960).
[31] G. E. Hutchinson, The paradox of the plankton, The American Naturalist **95**, 137 (1961).
[32] H. Ito and A. Sasaki, Evolutionary branching under multi-dimensional evolutionary constraints, Journal of Theoretical Biology **407**, 409 (2016).
[33] D. I. Bolnick and B. M. Fitzpatrick, Sympatric speciation: Models and empirical evidence, Annual Review of Ecology, Evolution, and Systematics **38**, 459 (2007).
[34] J. Coyne and H. Orr, *Speciation* (Sinauer, 2004).
[35] G. L. Bush, Sympatric speciation in animals: new wine in old bottles, Trends in Ecology & Evolution **9**, 285 (1994).
[36] B. G. Weiner, A. Posfai, and N. S. Wingreen, Spatial ecology of territorial populations, Proceedings of the National Academy of Sciences **116**, 17874 (2019).
[37] L. Pacciani-Mori, A. Giometto, S. Suweis, and A. Maritan, Dynamic metabolic adaptation can promote species coexistence in competitive microbial communities, PLOS Computational Biology **16**, 1 (2020).
[38] S. Louca and M. Doebeli, Calibration and analysis of genome-based models for microbial ecology, eLife **4**, e08208 (2015).
[39] . Nelson, David L. (David Lee), *Lehninger principles of biochemistry* (Fourth edition. New York : W.H. Freeman, 2005., 2005).
[40] S. Louca and M. Doebeli, Calibration and analysis of genome-based models for microbial ecology, eLife **4** (2015).
[41] O. Leimar, Multidimensional convergence stability (2009).
[42] A. Goyal and S. Maslov, Diversity, stability, and reproducibility in stochastically assembled microbial ecosystems, Phys. Rev. Lett. **120**, 158102 (2018).
[43] N. Shoresh, M. Hegreness, and R. Kishony, Evolution exacerbates the paradox of the plankton, Proceedings of the National Academy of Sciences **105**, 12365 (2008).
[44] É. Kisdi, Construction of multiple trade-offs to obtain arbitrary singularities of adaptive dynamics, Journal of Mathematical Biology **70**, 1093 (2015).
[45] E. Kisdi, Trade-off geometries and the adaptive dynamics of two co-evolving species, Evolutionary Ecology Research **8**, 959 (2006).
[46] J. Ma and S. A. Levin, The evolution of resource adaptation: How generalist and specialist consumers evolve, Bulletin of Mathematical Biology **68**, 1111 (2006).
[47] A. Erez, J. G. Lopez, B. G. Weiner, Y. Meir, and N. S. Wingreen, Nutrient levels and trade-offs control diversity in a serial dilution ecosystem, eLife **9**, e57790 (2020).
[48] E. Litchman, K. F. Edwards, and C. A. Klausmeier, Microbial resource utilization traits and trade-offs: implications for community structure, functioning, and biogeochemical impacts at present and in the future, Frontiers

in Microbiology **6**, 254 (2015).

Supplementary Material

SINGULAR POINTS AND THEIR CONVERGENCE AND EVOLUTIONARY STABILITY

We consider allocation strategies $\alpha = (\alpha_1, ..., \alpha_R)$ as in the main text, but here we assume a more general tradeoff function:

$$\sum_{j=1}^{R} b_j \alpha_j^{\gamma_j} = 1. \tag{S1}$$

It turns out to be convenient to reparametrize the strategy space as follows:

$$\beta_i \equiv b_j \alpha_j^{\gamma_j} \tag{S2}$$

for $j = 1, ..., R$. This simplifies the tradeoff expression to

$$\sum_{j=1}^{R} \beta_j = 1. \tag{S3}$$

Because the β_j increase monotonically with α_j, the adaptive dynamic properties in terms of convergence and evolutionary stability of singular points are the same for $\alpha = (\alpha_1, ..., \alpha_R)$- and $\beta = (\beta_1, ..., \beta_R)$-phenotypes. However, the tradeoff in β, eq. (S3), is linear, which simplifies the analysis.

In terms of β, the per capita rate of use of resource j of an individual with phenotype β is

$$\left(\frac{\beta_j}{b_j}\right)^{\frac{1}{\gamma_j}} r_j. \tag{S4}$$

(see eq. (1) in main text). We assume that nutrients are supplied to the system at a constant rate given by the vector $S = (S_1, S_2, \ldots, S_R)$, where S_j is the supply rate of the jth resource. We consider the low degradation rate regime, i.e., $\mu_j \to 0$ for all j in eq. (2) in the main text. Then the equilibrium population density of a population that is monomorphic in β becomes

$$n_\beta^* = \sum_{j=1}^{R} \frac{S_j}{d} \tag{S5}$$

(cf. eq. (4) in main text). The invasion fitness of a rare mutant with uptake strategy β' in a resident β at ecological equilibrium n_β^* becomes:

$$f(\beta, \beta') = \sum_{j=1}^{R} \left(\frac{\beta_j'}{\beta_j}\right)^{1/\gamma_j} \frac{S_j}{n_\beta^*} - d. \tag{S6}$$

To derive the adaptive dynamics of β, we calculate the selection gradient $q(\beta) = (q_1(\beta), ..., q_R(\beta))$ and project it on to the linear constraint space:

$$q_j(\beta) = \left.\frac{\partial f(\beta, \beta')}{\partial \beta_j'}\right|_{\beta'=\beta} = \frac{S_j}{\beta_j \gamma_j n_\beta^*} \tag{S7}$$

$$\frac{d\beta_j}{dt} = \sigma n_\beta^* \left(q_j(\beta) - \frac{1}{R}\sum_{k=1}^{R} q_k(\beta)\right) = \sigma n_\beta^* \left(\frac{S_j}{\beta_j \gamma_j n_\beta^*} - \frac{1}{R}\sum_{k=1}^{R} \frac{S_k}{\beta_k \gamma_k n_\beta^*}\right). \tag{S8}$$

Here the term

$$\frac{1}{R}\sum_{k=1}^{R} q_k(\beta) = \frac{1}{R}\sum_{k=1}^{R} \frac{S_k}{\beta_k \gamma_k n_\beta^*} \tag{S9}$$

is the component of the selection gradient (S7) that is orthogonal to the tradeoff hyperplane (note that $(1/\sqrt{R}, \ldots, 1/\sqrt{R})$ is a unit vector orthogonal to the tradeoff hyperplane).

As in the main text we set the mutational parameter $\sigma = 1$, hence the adaptive dynamics of β becomes:

$$\frac{d\beta_j}{dt} = \frac{S_j}{\beta_j \gamma_j} - \frac{1}{R}\sum_{k=1}^{R} \frac{S_k}{\beta_k \gamma_k}. \tag{S10}$$

Note that we only need $R-1$ equations due to the (linear) tradeoff. It is easy to see that (S10) has a unique fixed point, i.e., there is a unique singular point for the adaptive dynamics given by:

$$\beta_j^* = \frac{S_j/\gamma_j}{\sum_{k=1}^{R} S_k/\gamma_k} \tag{S11}$$

for $j = 1, ..., R$. In terms of the original trait α, (S11) is eq. (8) in the main text.

To check for convergence stability of $\beta^* = (\beta_1^*, ..., \beta_R^*)$, we have to calculate the Jacobian matrix J of the right hand side of (S10), evaluated at the singular point β^*. It is easy to see that the jk-th element of J is

$$J_{jk} = -\delta_{jk}\frac{S_j}{\gamma_j \beta_j^{*2}} + \frac{1}{R}\frac{S_k}{\gamma_k \beta_k^{*2}}. \tag{S12}$$

Thus, J is of the form

$$J = J_d + A, \tag{S13}$$

where J_d is a diagonal matrix with element $J_{jj} = \frac{S_j}{\gamma_j \beta_j^{*2}}$, and A is a matrix whose elements in the k-th column are all identical and equal to $\frac{1}{R}\frac{S_k}{\gamma_k \beta_k^{*2}}$. This implies that the matrix A maps any vector in phenotype space to a vector that is orthogonal to the tradeoff hyperplane (i.e., to a multiple of the vector $(1, ..., 1)$). If $\Delta\beta = (\Delta\beta_1, \ldots, \Delta\beta_R)$ is any vector of deviations from the singular point, it follows that the projection of $J\Delta\beta$ onto the tradeoff hyperplane is the same as the projection of the vector $J_d\Delta\beta$. Since all eigenvalues of J_d are real and negative, it follows that the singular point β^* is a local attractor, i.e., convergent stable, regardless of the exponents γ_j, $j = 1, ..., R$.

For evolutionary stability, we have to calculate the Hessian matrix H of second derivatives of the invasion fitness function, (S6), with respect to the mutant trait β' and evaluated at the singular trait value β^*. The jk-th element of H is

$$H_{jk} \equiv \left.\frac{\partial^2 f}{\partial\beta_j' \partial\beta_k'}\right|_{\beta'=\beta=\beta^*} = \delta_{jk}\nu\frac{1-\gamma_j}{S_j}, \tag{S14}$$

were ν is a constant:

$$\nu = d\frac{\left(\sum_{l=1}^{R} S_l/\gamma_l\right)^2}{\sum_{m=1}^{R} S_m}. \tag{S15}$$

Thus, H is diagonal (due to the transformation from α to β), and H is negative definite, i.e., all eigenvalues are < 0, if and only if $\gamma_j > 1$ for all $j = 1, ..., R$. Because the tradeoff hyperplane is linear in β, it follows that any index j with $\gamma_j < 1$ provides a branching direction β_j, i.e., a direction in phenotype space along which evolutionary diversification is possible. More precisely, any direction in β-space (other than orthogonal to the tradeoff surface) along which the unconstrained Hessian (S14) has a minimum corresponds to a direction on the tradeoff surface along which diversification is possible.

The results presented in the main text now follow from the above by setting $\gamma_j = \gamma$ for $j = 1, ..., R$. But the above analysis also suggests that with suitably chosen γ_j, it is possible to generate evolutionary branching in some directions, but not in others. This is illustrated in Figures S1 and S2. Fig. S1 illustrates diversification in the direction of α_3 ($\gamma_3 < 1$) without diversification in the directions α_1 and α_2 ($\gamma_1, \gamma_2 > 1$).

Fig. S2 illustrates diversification in the directions α_1 and α_2 ($\gamma_1, \gamma_2 < 1$), with no diversification in α_3 ($\gamma_3 > 1$).

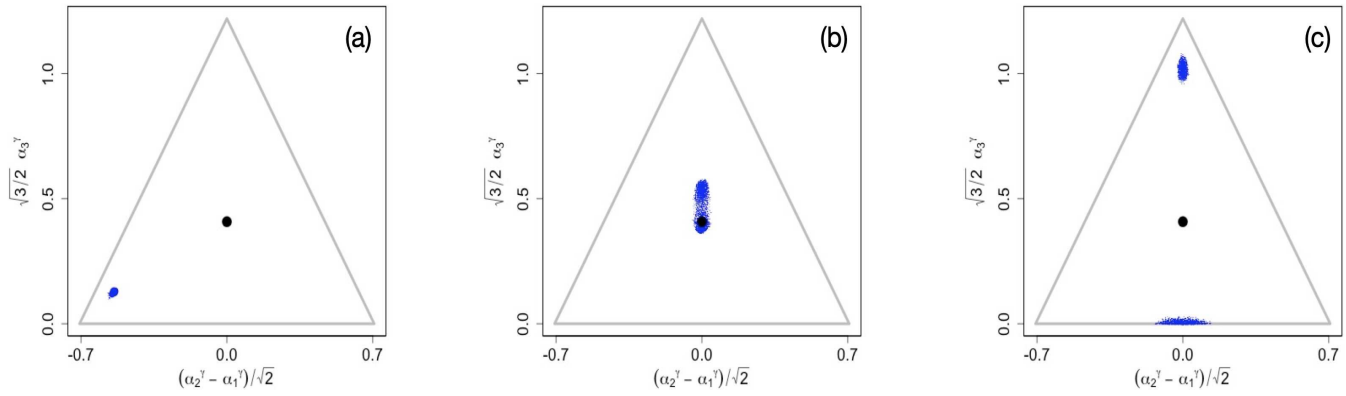

FIG. S1: Example of evolutionary dynamics for $\gamma_1 = \gamma_2 = 1.1$ and $\gamma_3 = 0.9$, showing convergence to the singular point and subsequent diversification only in the α_3 direction. (Note that the dynamics are shown in the original α-phenotype space.) The corresponding video can be found here, each frame in the video is separated by 2000 time steps. Other parameter values were $S_j = 1$, $\mu_j K_j = 0.1$ for $j = 1, 2, 3$, and $d = 0.25$.

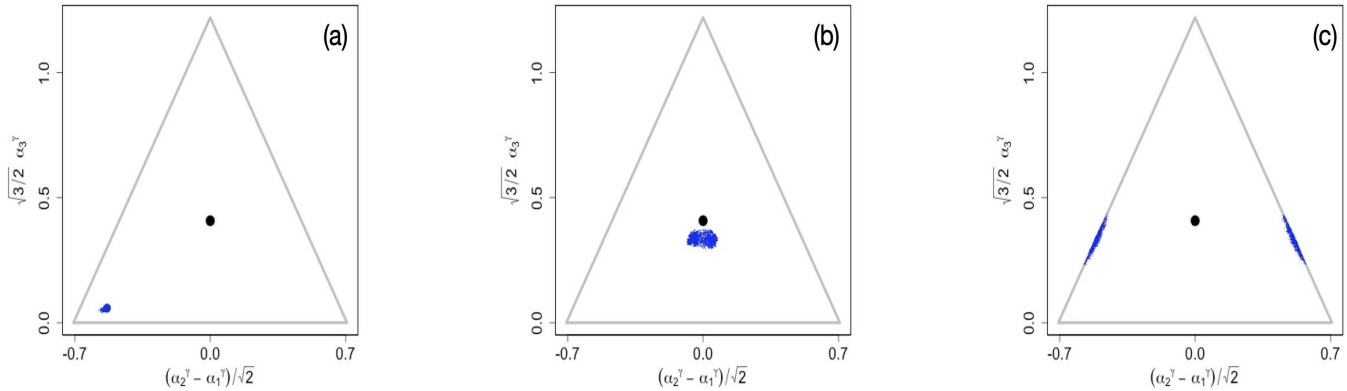

FIG. S2: Example of evolutionary dynamics for $\gamma_1 = \gamma_2 = 0.9$ and $\gamma_3 = 1.2$, showing convergence to the singular point and subsequent diversification only in $\alpha_1 - \alpha_2$ directions. (Note that the dynamics are shown in the original α-phenotype space.) The corresponding video can be found here, each frame in the video is separated by 2000 time steps. Other parameter values were $S_j = 1$, $\mu_j K_j = 0.1$ for $j = 1, 2, 3$, and $d = 0.25$.

MAINTENANCE OF DIVERSITY IN ECOLOGICAL TIME SCALES

Here we briefly show how nonlinear trade-offs affect diversity on ecological time scale. To do this, we initiate the simulations with a set of e.g. randomly chosen phenotypes throughout phenotype space and then run the systems with the mutational process turned off. Figure S3A shows the initial configuration used for three different scenarios with different exponents γ of the tradeoff (here we again assume that $\gamma_j = \gamma$ for all j). The functional form of the tradeoffs has a profound effect on the number of surviving species, with many species coexisting when $\gamma = 1$, as reported in [1], (Figure S3B), but with typically only R species surviving when $\gamma < 1$ (S3C)and only very few species surviving in the close vicinity of the singular point when $\gamma > 1$ (S3D).

[1] A. Posfai, T. Taillefumier, and N. S. Wingreen, Phys. Rev. Lett. **118**, 028103 (2017).

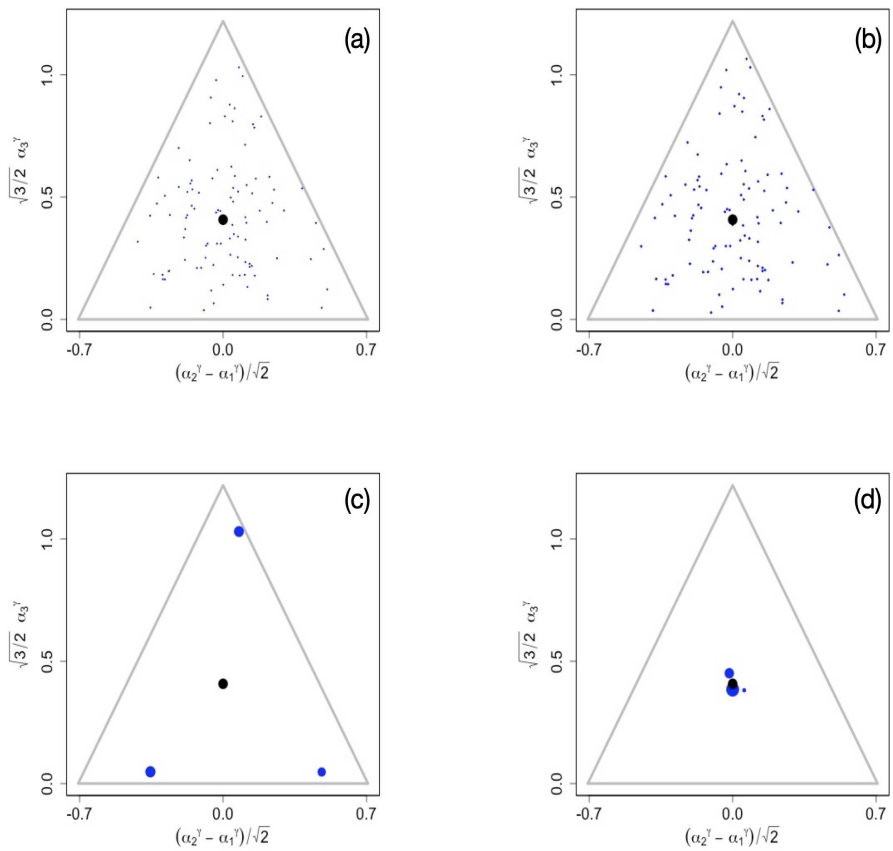

FIG. S3: Initial population configuration of 100 randomly placed clusters in the phenotypic simplex (A), final configurations after 5000000 time units for $\gamma = 1$ (B), $\gamma = 0.9$ (C) and $\gamma = 1.1$ (D). Videos of the entire evolutionary processes can be found **here**, time interval between frames increased as a geometric progression, $t(i+1) = 1.05t(i)$. Other parameter values were $S_j = 1$, $\mu_j K_j = 0.1$ for $j = 1, 2, 3$, and $d = 0.25$.